



OPEN ACCESS

Original research

Role of CNNM4 in the progression of cholangiocarcinoma: implications for ferroptosis and therapeutic potential

Maria Mercado-Gómez ¹, Naroa Goikoetxea-Usandizaga,^{1,2} Alvaro Eguileor Giné,¹ Miguel A Merlos Rodrigo,³ Marta Bento Afonso,⁴ Mikel Azkargorta,⁵ Leidy Estefanía Zapata-Pavas,¹ Claudia M Rejano-Gordillo,¹ Marta R Romero,^{2,6} Isabel Mendizabal,^{7,8} Pedro M Rodrigues,^{2,8,9} Hanghang Wu,¹⁰ Rubén Rodríguez-Agudo,¹ Marina Serrano-Maciá,¹ Paula Olaizola,⁹ Jon Ander Barrenechea-Barrenechea,¹ Irene González Recio,¹ Maite G Fernandez-Barrena ^{2,11}, Diletta Overi ¹², Eugenio Gaudio,¹² Ute Schaeper,¹³ Saioa Garcia-Longarte ⁷, Mariana Yáñez-Bartolomé,^{14,15} Patricia Peña-SanFelix,¹ Clàudia Gil-Pitarch,¹ Ainhoa Lapitz,⁹ Hana Michalkova,³ Zbynek Heger,³ Carolina Conter,¹ Rocío I R Macias ^{2,6}, Arkaitz Carracedo,^{7,8} Jesús Bañales,^{2,8,9,16} Víctor Moreno ¹⁷, Angela Lamarca,¹⁸ Rajat Singh,^{19,20} Teresa Cardoso Delgado,¹ Luis Alfonso Martínez-Cruz,¹ Felix Elortza,²¹ Matias A Avila ^{2,11}, César Martín,²² Tian V. Tian ^{14,15}, Teresa Macarulla,^{14,15} Daniela Buccella,²³ Francisco Javier Cubero ^{2,10}, Diego F Calvisi,^{24,25} Guido Carpino ¹², Jose J G Marin ^{2,6}, Cecília M P Rodrigues,⁴ Maria Luz Martinez-Chantar ^{1,2}

► Additional supplemental material is published online only. To view, please visit the journal online (<https://doi.org/10.1136/gutjnl-2024-333255>).

For numbered affiliations see end of article.

Correspondence to

Maria Luz Martinez-Chantar; mlmartinez@cicbiogune.es

MM-G and NG-U contributed equally.

Received 9 July 2024

Accepted 6 February 2025



► <https://doi.org/10.1136/gutjnl-2024-333061>



© Author(s) (or their employer(s)) 2025. Re-use permitted under CC BY-NC. No commercial re-use. See rights and permissions. Published by BMJ Group.

To cite: Mercado-Gómez M, Goikoetxea-Usandizaga N, Giné AE, et al. *Gut* Epub ahead of print: [please include Day Month Year]. doi:10.1136/gutjnl-2024-333255

ABSTRACT

Background and objective Cholangiocarcinoma (CCA) is a heterogeneous neoplasm of the biliary epithelium that easily infiltrates, metastasises and recurs. Magnesium disbalance is a hallmark of CCA, with the magnesium transporter cyclin M4 (CNNM4) being a key driver of various hepatic diseases. This study aims to unravel the role of CNNM4 in the initiation and progression of CCA.

Design CNNM4 protein and gene expression were assessed in vitro, in vivo and in patients with CCA. Silencing of *CNNM4* was effectively achieved by using small interfering RNA (siRNA) or short hairpin RNA in CCA cell lines and GalNAc-conjugated siRNA in a transposon-based CCA mice model. The impact of CNNM4 on tumour cell proliferation, migration and invasion to the lungs was evaluated using the chicken chorioallantoic membrane model. Proteomic analysis was employed to elucidate the underlying molecular mechanisms.

Results CNNM4 was upregulated in CCA samples from humans, mice and cell lines. Functional studies demonstrated that CNNM4 deficiency attenuates cell growth, chemoresistance, migration, invasion, cancer stem cell properties and Warburg effect in vitro and in vivo. Proteomic analysis identified nuclear protein 1 as an upstream regulator of CNNM4-induced ferroptosis in CCA, ultimately leading to cell death. The iron chelator deferiprone could reverse the decreased proliferation induced by *CNNM4* silencing, while inhibition of the heme oxygenase-1 by zinc protoporphyrin IX affected only

WHAT IS ALREADY KNOWN ON THIS TOPIC

⇒ Maintaining magnesium ion (Mg²⁺) homeostasis is crucial for various physiological processes. The Mg²⁺ transporter cyclin M4 (CNNM4) has emerged as a key player in liver diseases such as metabolic dysfunction-associated steatotic liver disease (NAFLD) and drug induced liver injury (DILI).

WHAT THIS STUDY ADDS

⇒ Silencing *CNNM4* is a potential new therapy for cholangiocarcinoma by slowing cancer growth and reversing key cancer hallmarks through ferroptosis-induced reactive oxygen species production.

HOW THIS STUDY MIGHT AFFECT RESEARCH, PRACTICE OR POLICY

⇒ Inhibition of CNNM4 emerges as a promising therapeutic strategy for patients with cholangiocarcinoma, a highly aggressive and recurrent neoplasm, as it effectively limits tumour proliferation, sensitises cells to chemotherapy and halts metastasis.

the growth of cells with no targeted *CNNM4* inhibition, highlighting the specificity of ferroptosis in CNNM4-associated effects.

Conclusion This study reveals that increased CNNM4 expression drives CCA progression and malignancy and that its inhibition may be an effective therapeutic strategy to limit proliferation and metastasis in patients with CCA.

INTRODUCTION

Cholangiocarcinoma (CCA), a rare and diverse cancer affecting the biliary tree, poses a significant challenge in the field of oncology. According to the anatomical location of the tumour, CCA can be categorised into intrahepatic (iCCA) and extrahepatic (eCCA), further divided into perihilar or distal based on its anatomical origin.¹ It is characterised by a poor prognosis, with a 5-year overall survival (OS) <10% postdiagnosis.^{1,2} Complete surgical resection remains the only potential cure for iCCA, but only 20–30% of patients present with resectable disease. Even after curative-intent surgical resection, the 5-year OS rate is approximately 20–35%.³ Key factors contributing to this challenging situation comprise its aggressive nature, delayed diagnosis and resistance to chemotherapy. Hence, despite progress in biomedicine, there remains a pressing need for more effective treatments for CCA.

A promising approach to tackle CCA involves modulation of ferroptosis, a regulated non-apoptotic cell death driven by iron-dependent lipid peroxidation. Studies indicate that inhibitors targeting mutant isocitrate dehydrogenase 1 (mutant IDH1), used in treating advanced unresectable iCCA with *IDH1* mutations, sensitise tumour cells to ferroptosis, reducing proliferation, invasion and metastasis.⁴ Oxidative stress is a crucial feature in ferroptosis, with glutathione peroxidase 4 (GPX4) acting as the central repressor of ferroptosis using reducing power from reduced glutathione (GSH), the synthesis of which is dependent on SLC7A11, to transform reactive polyunsaturated fatty acid-phospholipid (PUFA-PL)-OOH into non-lethal PUFA-PL-OH. Iron-dependent enzymes like arachidonate lipoxygenases (ALOXs) and cytochrome P450 oxidoreductase oxidise PUFA-PLs, compromising plasma membrane integrity and leading to toxic aldehydes.^{5,6} Increasing evidence suggests that the inactivation of nuclear protein 1 (NUPR-1) impairs mitochondrial function and energy metabolism in cancer cells and triggers ferroptosis via iron metabolism, reactive oxygen species (ROS) homeostasis and the GSH/GPX4 pathway.^{7,8} While magnesium (Mg) combined with isoglycyrrhizinate attenuates liver fibrosis through ferroptosis induction, the role of Mg ion (Mg²⁺) alone in promoting ferroptosis is yet to be understood.⁹

Mg²⁺, a cofactor in over 300 enzymatic reactions, is essential for physiological homeostasis, regulating key processes like DNA repair, genomic stability, signal transduction, cell proliferation and apoptosis.^{10–12} Mg²⁺ deficiency in the liver has been linked to immune and inflammatory disruptions, potentially promoting carcinogenesis.^{13,14} Therefore, rebalancing hepatic Mg²⁺ appears promising for treating biliary-related conditions.

The regulation of Mg²⁺ transport across cellular membranes involves multiple transporters, including the CNNM family. Cyclin M3 (CNNM3) and CNNM4 are implicated in cancer progression and other liver-related pathologies.^{15–18} However, their specific role in bile duct pathobiology remains unexplored.

We found that of the four CNNM isoforms, CNNM4 was the only one consistently found to have increased expression in both human and experimental CCA samples. To explore its implication in cholangiocarcinogenesis and assess the therapeutic potential of silencing CNNM4, we performed experiments in CCA rodent models, the chick chorioallantoic membrane (CAM) and

tumour cell lines. Suppression of CNNM4 levels reverted key cancer hallmarks, including proliferation, drug resistance, the Warburg effect, stem-like characteristics and crucial metastatic steps. Finally, our results revealed the mechanism of action of CNNM4 through ferroptosis, suggesting it is a potential therapeutic target for CCA via Mg²⁺ transport modulation.

MATERIAL AND METHODS

Human and organoid samples

CCA and control tissues (surrounding liver or normal bile ducts) from eight independent cohorts of patients were studied at the transcriptomic level. The research protocol was approved by their respective ethics committees and all patients signed written consent forms allowing the use of their samples for biomedical research. Expanded information is shown in online supplemental methods.

Disease models

CCA sleeping beauty and in vitro models were generated and employed as described in the online supplemental methods.

RESULTS

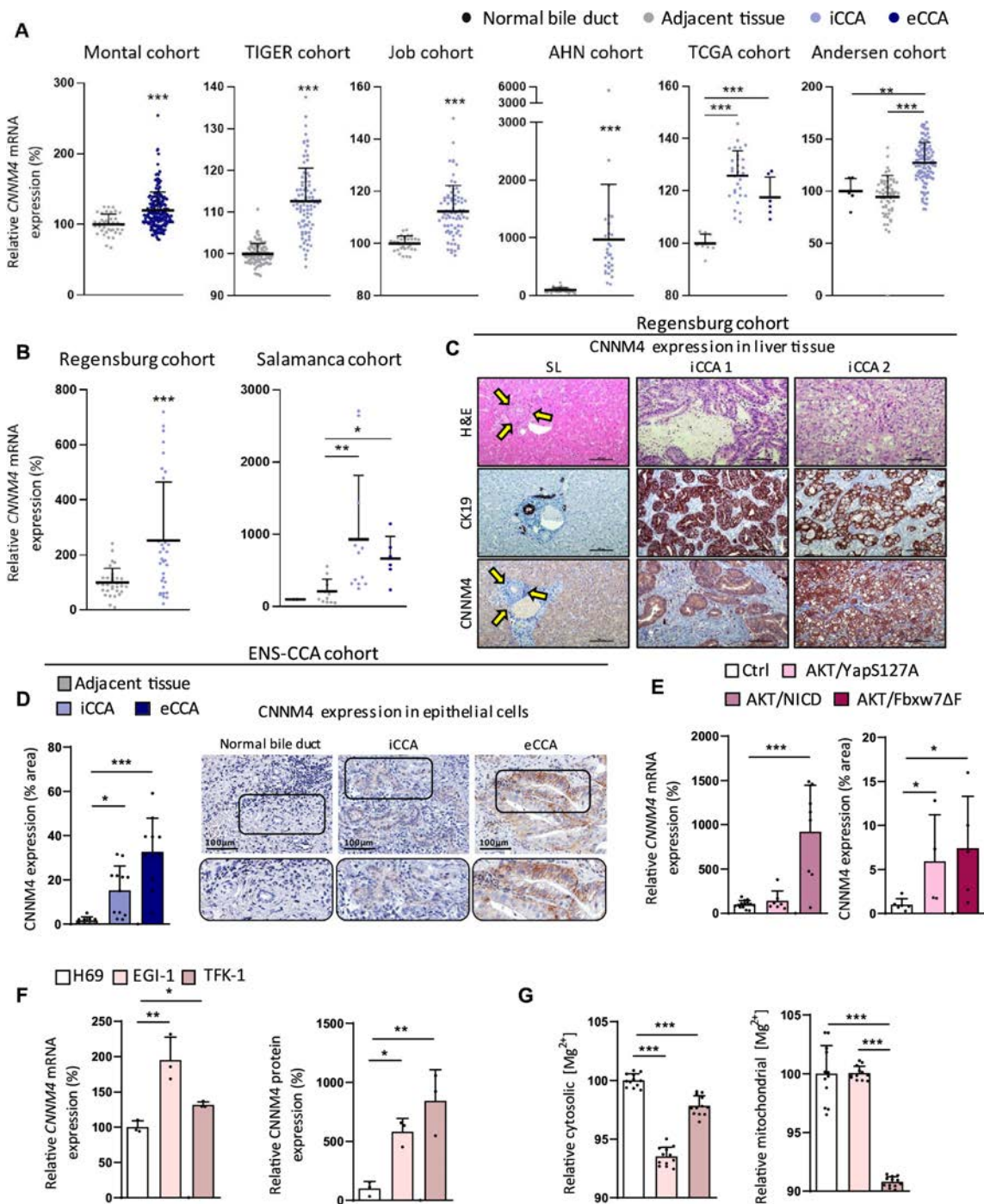
CNNM4 is upregulated in clinical CCA cases and experimental mouse model

Our previous findings have highlighted CNNM4's critical role in the progression of various liver diseases.^{17,18} To assess its involvement in CCA, we examined expression data from eight independent cohorts of patients comparing resected CCA samples (both iCCA and eCCA) with controls (either normal bile ducts or adjacent liver tissues). *CNNM4* expression exhibited a consistent increase in CCA tumour samples across all cohorts, in comparison to control samples, regardless of their anatomical subtype (figure 1A,B). Conversely, the expression of *CNNM1–3* did not show consistent patterns in those databases, emphasising CNNM4's specificity (online supplemental figure S1A). *CNNM4* exhibited higher upregulation in CCA than all the diverse tumour types documented in The Cancer Genome Atlas database (online supplemental figure S1B).

Immunohistochemical analysis demonstrated minimal CNNM4 immunoreactivity in non-tumorous tissues but a robust expression in CCA samples (figure 1C,D and online supplemental figure S2A). Although CNNM4 was exclusively detected within the tumour, its presence is not restricted to epithelial cancerous cells, as it is also detected in stromal cells in tissues with both low and high CNNM4 expression (online supplemental figure S2B). In samples from patients with iCCA and eCCA, CNNM4 was positively correlated with number of von Willebrand Factor-positive microvessels and with the proliferation index calculated by immunohistochemistry for proliferating cell nuclear antigen (online supplemental figure S2C).

Murine 'sleeping beauty' models of CCA supported CNNM4's role, with its overexpression transcriptionally confirmed in the AKT/notch intracellular domain model and histological analyses in tissues of the AKT/YapS127A and AKT/Fbxw7ΔF mice models (figure 1E and online supplemental figure S2D).^{19–21} Moreover, in a database that compares healthy hepatic organoids with organoids derived from patients with CCA, the tumour-derived organoids exhibited higher expression of *CNNM4* (online supplemental figure S2E).

To determine whether changes in *CNNM4* expression are altered at the cellular level as well, we used two human CCA cell lines (EGI-1 and TFK-1) and the non-tumorous immortalised cholangiocyte cell line H69. Analysis revealed elevated



(Mercado-Gómez M., et al.)

Figure 1 *CNNM4* overexpression in patients with CCA, preclinical models and cell lines. (A) *CNNM4* mRNA expression in CCA relative to normal bile duct and/or adjacent non-tumour liver from the Montal, TIGER, Job, Ahn, TCGA and Andersen microarray and RNA-seq cohorts. (B) *CNNM4* mRNA expression in CCA relative to adjacent liver in Regensburg and Salamanca RT-qPCR cohorts. (C) *CNNM4* immunoreactivity in human non-tumorous (normal biliary cells indicated by arrows) and iCCA from the Regensburg cohort. CK19 staining indicates benign and malignant biliary cells. Magnification: 200 \times ; scale bar: 100 μ m. (D) *CNNM4* immunoreactive in healthy bile duct, iCCA and eCCA from the ENS-CCA cohort. Magnification: 400 \times ; scale bar: 100 μ m. (E) Transcriptional (left) and immunohistochemical (right) *CNNM4* expression in transposon-based mouse models of CCA. (F) Transcriptional (left) and immunohistochemical (right) *CNNM4* expression in CCA cell lines compared with a healthy human cholangiocyte cell line (H69). (G) Relative intracellular magnesium levels in normal human cholangiocytes (H69) and CCA cell lines (EGI-1 and TFK-1) using cytosolic (left) and mitochondrial (right) labelling. One-way ANOVA, Kruskal-Wallis, Wilcoxon, Mann-Whitney and paired/unpaired Student's t-test were used depending on the normality of the samples. Error bars represent SD and asterisks indicate p values (* <0.05 , ** <0.01 and *** <0.001). ANOVA, analysis of variance; CCA, cholangiocarcinoma; CK19, cytokeratin 19; *CNNM4*, cyclin M4; eCCA, extrahepatic cholangiocarcinoma; ENS-CCA, European Network for the Study of Cholangiocarcinoma; iCCA, intrahepatic cholangiocarcinoma; Mg^{2+} , magnesium ion; mRNA, messenger RNA; NICD, notch intracellular domain; RT-qPCR, reverse-transcription quantitative PCR; SL, surrounding tissue; TCGA, The Cancer Genome Atlas; TIGER, The Thailand Initiative in Genomics and Expression Research.

CNNM4 expression in the CCA cell lines compared with H69, at both messenger RNA (mRNA) and protein levels (figure 1F and online supplemental figure S2F). Furthermore, intracellular Mg^{2+} levels decreased in the cytoplasm of CCA cell lines compared with control cells, and within the TFK-1 cell line's mitochondria, evidencing *CNNM4*'s role in Mg^{2+} extrusion in CCA (figure 1G).

These findings indicate that increased *CNNM4* levels are a common characteristic in patients with CCA, irrespective of the anatomical subtype.

Silencing *CNNM4* reduces tumour aggressiveness in CCA cell lines through modulation of its magnesium efflux activity

Given *CNNM4*'s potential role in cholangiocarcinogenesis, we investigated its impact on human CCA cell lines by silencing *CNNM4* using five different short hairpin RNAs (shRNAs) and a control shRNA. Notably, shRNA2 (sh2) and shRNA5 (sh5) exhibited more potent silencing effects (data not shown), so they were those used in upcoming experiments (figure 2A and online supplemental figure S3A). Noteworthy, a decrease in *CNNM4* mRNA expression was observed, mirroring the protein changes, while the expression of the other Mg^{2+} transporters remained unaltered (online supplemental figure S3B). *CNNM4* small interfering RNA (siRNA) was employed in an intrahepatic CCA cell line to validate the anatomically independent role of *CNNM4* (online supplemental figure S3C). Further, using selective probes, we detected that the cytoplasmic and mitochondrial Mg^{2+} levels were increased in cell lines in which *CNNM4* was silenced (figure 2B,C and online supplemental figure S3D).^{18 22}

The silencing of *CNNM4* expression reduced cell proliferation in all CCA cell lines, as indicated by crystal violet staining assay (figure 2D and online supplemental figure S3E). Conversely, siRNA-mediated *CNNM4* silencing did not affect the growth rate of the non-tumorous cholangiocyte cell line H69 and the healthy human hepatocyte cell line THLE-2 (online supplemental figure 3E,F).

To assess the role of Mg^{2+} in this phenomenon, we increased its concentration from the baseline of 1 mM to 5 mM in both cell lines. Such supplementation did not alter cell proliferation, emphasising the distinctive impact of *CNNM4* (online supplemental figure S3G). Furthermore, overexpression of the T495I mutant form of *CNNM4*, which competes with endogenous *CNNM4* for Mg^{2+} binding, leads to a significant reduction in CCA cell proliferation in EGI-1 and Huh28 cells (online supplemental figure S4A,B).¹⁷ Finally, these results were supported by the observed lack of Mg^{2+} efflux under these experimental conditions (online supplemental figure S4C,D). These findings demonstrate that the observed effects of *CNNM4* are closely associated with its Mg efflux activity.

Silencing *CNNM4* in CCA enhances drug sensitivity and triggers metabolic rewiring with loss of stemness

Considering the effect on proliferation, we aimed to study whether silencing *CNNM4* would increase sensitivity to the common CCA chemotherapeutic agents (cisplatin, doxorubicin, gemcitabine and 5-fluorouracil) in CCA. Exposure of EGI-1 and TFK-1 cells to these agents revealed increased sensitivity when *CNNM4* was silenced (figure 2E). This altered sensitivity was reflected in changes in expression of genes associated with mechanisms of chemoresistance, indicating an involvement of *CNNM4* in chemoresistant phenotype of CCA (online supplemental figure S4E).

Metabolic reprogramming has been shown to enhance sensitivity increasing mitochondrial oxidative stress in CCA.²³ To evaluate energetic metabolism dependency, 2-deoxy-D-glucose, a competitive inhibitor of glycolysis, was administered to the CCA lines, which resulted in a reduced proliferation with baseline *CNNM4* levels, indicating a greater reliance on glycolysis compared with cells with *CNNM4* silencing (figure 2F). In addition, CCA cells with silenced *CNNM4* exhibited decreased levels of extracellular lactate (figure 2G). This finding was confirmed by measuring basal glycolysis and the change in oxygen consumption rate (OCR) relative to extracellular acidification rate (ECAR) in stable TFK-1 cells and HuH-28 cells (figure 2H,I and online supplemental figure S4F,G).

Cancer stem cells (CSCs) sustain malignant traits and treatment resistance, with recent evidence highlighting the crucial role of mitochondrial-dependent metabolism in maintaining CCA stemness.²⁴ In the three-dimensional (3D) CCA cell culture model (hanging drop spheroids), *CNNM4* silencing impaired the formation of these structures in both EGI-1 and TFK-1 cells at 72 hours (figure 2J). In a different 3D spheroid model, where CSCs or cells with stem cell-related characteristics are enriched, *CNNM4*-silenced cells produced fewer spheres than control cells after 14 days (figure 2K and online supplemental figure S4H,I). In line with this, spheroids derived from *CNNM4*-silenced CCA cells showed reduced expression of CSC markers (online supplemental figure S4J).

In summary, inhibiting *CNNM4* in CCA cell culture decreases cell index and results in a less dependent on glycolysis with fewer CSCs and sensitises these cells to chemotherapy agents.

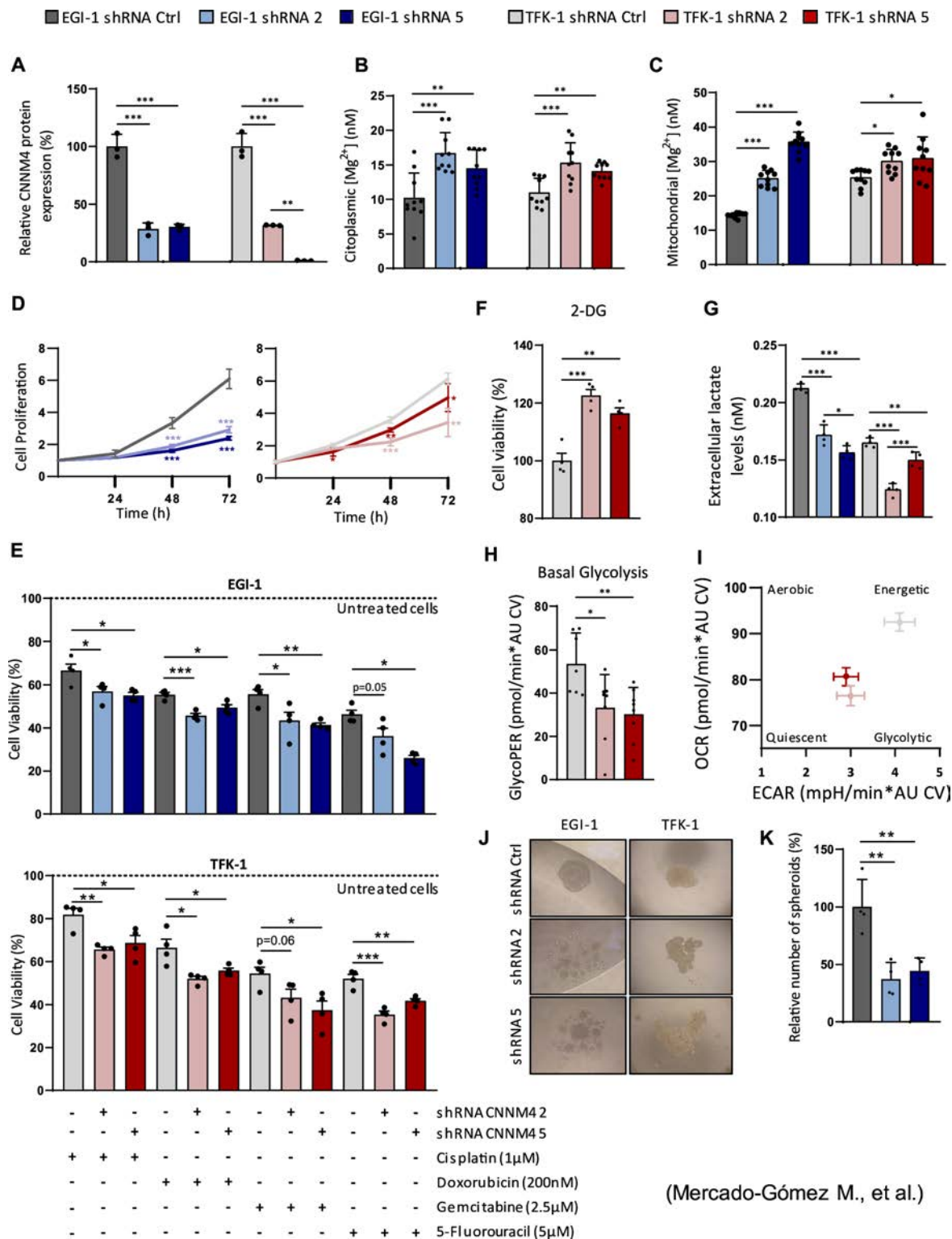
CNNM4 knock-down reduces tumour growth, invasion and metastatic potential of cholangiocarcinoma cells in the CAM assay

CCA is usually diagnosed in advanced stages, with presence of distant metastasis, implying a very poor prognosis. Common sites of metastasis include lymph nodes, peritoneum and liver, with occasional occurrences in the lungs and bones.²⁵ In the TGCA database, we found a positive association between *CNNM4* levels and vascular invasion (figure 3A). Additionally, the Regensburg cohort showed an almost significant association between *CNNM4* mRNA expression and lung metastasis, with no observed variation in node metastasis (figure 3B).

To explore the link between *CNNM4* and the metastatic process, we employed a well-established model: the *ex ovo* and *in ovo* CAM. Silencing of *CNNM4* dramatically suppressed tumour growth compared with the control group (online supplemental figure S5A). Only cells transfected with control shRNA exhibited profound migration to adjacent CAM (online supplemental figure S5B).

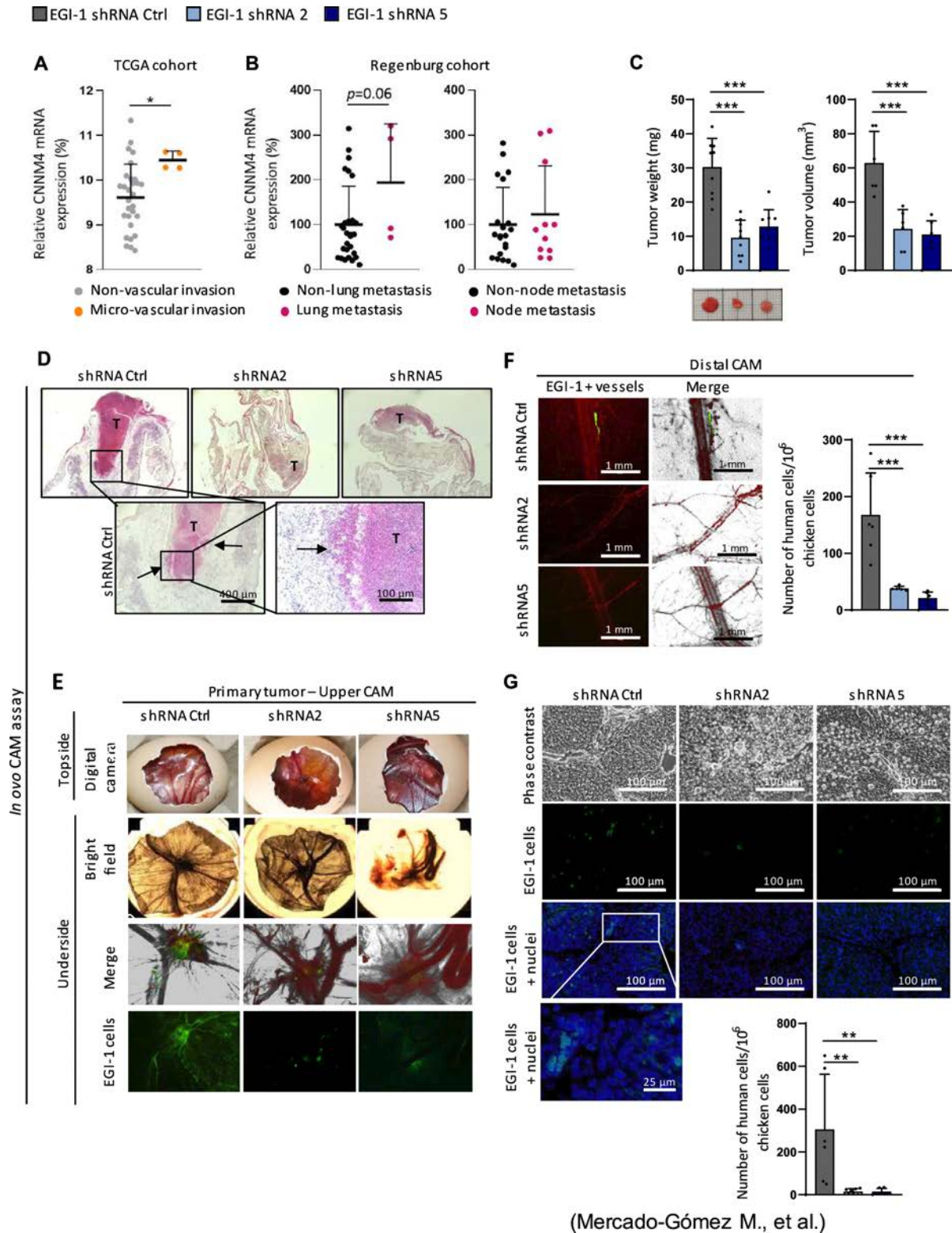
We then focused on exploring *CNNM4*'s role in crucial metastatic stages including intravasation, circulatory migration, extravasation and organ invasion. Tumour growth was assessed through weight and volume measurements and total EGI-1 cell counts in the distal CAM and lungs of the embryos. Cells with silenced *CNNM4* displayed a significant twofold reduction in the weight and volume of primary tumours compared with the control (figure 3C). Histopathological examination of excised tumours revealed substantial invasion of cells transfected with shRNA Ctrl into the underlying CAM tissue, a phenomenon not observed in the absence of *CNNM4* (figure 3D).

In the *in ovo* experimental settings, silencing *CNNM4* led to a notable reduction in tumour growth (figure 3E). Furthermore, analysis of cells migrating into the distal CAM showed a marked



(Mercado-Gómez M., et al.)

Figure 2 *CNNM4* silencing reduces proliferation, chemoresistance, glycolysis and spheroid formation in CCA cell lines. (A) Relative CNNM4 protein expression in *CNNM4*-silenced EGI-1 and TFK-1 cell lines (n=3). Intracellular magnesium determination using cytosolic (B) and mitochondrial (C) labelling in stable *CNNM4*-silenced cells compared with control cells (n=10). (D) Proliferation assessed by crystal violet staining. (E) Cell viability in cisplatin, doxorubicin, gemcitabine and 5-fluorouracil-treated EGI-1 and TFK-1 cells with baseline or silenced *CNNM4* levels (n=4) evaluated by crystal violet assay. (F) Cell viability of *CNNM4*-silenced or control TFK-1 cells after 2-deoxy-D-glucose administration (n=4). (G) Extracellular lactate concentration of CCA cell lines with silencing of CNNM4 or with CNNM4 baseline levels (n=4). Results from the seahorse technique showing basal glycolysis (H, n=8) and OCR/ECAR in TFK-1 cells (I, n=8). Hanging drop spheroid formation at 48 hours (J) and CSC-enriched spheroid formation after 14 days (K) in CCA cell lines with baseline or silenced *CNNM4* levels (n=4). Statistical significance assessed using one-way ANOVA and Student's t-test. Error bars represent SD and asterisks indicate p values (*<0.05, **<0.01 and ***<0.001). ANOVA, analysis of variance; AU CV, arbitrary units from crystal violet quantification; CCA, cholangiocarcinoma; CNNM4, cyclin M4; CSC, cancer stem cell; 2-DG, 2-deoxy-D-glucose; ECAR, extracellular acidification rate; GlycoPER, glycolytic proton efflux rate; Mg^{2+} , magnesium ion; OCR, oxygen consumption rate; shRNA, short hairpin RNA.



(Mercado-Gómez M., et al.)

Figure 3 Inhibitory effects of *CNNM4* silencing on EGI-1 tumour development and invasion by *in ovo* CAM model. *CNNM4* expression in TCGA cohort patients based on vascular invasion (A) and in the Regensburg cohort grouped by lung (left) and node metastasis (right) (B). (C) Representative photographs of excised EGI-1 tumours, tumour weights (n=9) and volumes (n=6) from *in ovo* CAM assay. (D) Representative micrographs of tumours sections stained with H&E. Arrows indicate sites of tumour invasion into CAM after shRNA Ctrl transfection. (E) Fluorescence micrographs showing inhibitory effects of *CNNM4* silencing on EGI-1 cells intravasation to the adjacent CAM. (F) Representative micrographs showing EGI-1 cells in the vasculature in the distal CAM and q-PCR quantitation of EGI-1 cell spread to distal CAM. (G) Fluorescence micrographs showing inhibitory effects of *CNNM4* silencing on metastatic spread of EGI-1 cells to lungs and q-PCR quantitation of EGI-1 cells spread to lungs. One-way ANOVA, Mann-Whitney and unpaired Student's t-test were used depending on the normality of the samples. Error bars represent SD and asterisks indicate p values (* <0.05 , ** <0.01 and *** <0.001). ANOVA, analysis of variance; CAM, chorioallantoic membrane; *CNNM4*, cyclin M4; mRNA, messenger RNA; q-PCR, quantitative PCR; shRNA, short hairpin RNA; T, tumour area; TCGA, The Cancer Genome Atlas.

decrease in intravasation in the absence of *CNNM4* (figure 3F). Additionally, examination of extravasation and invasion into the lungs revealed a significant inhibitory effect on these processes due to shRNA-mediated silencing of *CNNM4*. This effect was supported by q-PCR quantification of EGI-1 cells in excised lung tissues (figure 3G).

According to these data, *CNNM4* may play a role in the induction of metastasis and could be an important factor in cholangiocarcinogenesis.

Inhibition of NUPR-1 following *CNNM4* silencing enhances ferroptosis in CCA cells

To further understand the underlying mechanisms of silencing *CNNM4* in CCA tumour growth, we characterised the proteomic changes in EGI-1 and TFK-1 cells after *CNNM4* silencing using liquid chromatography coupled to tandem mass spectrometry.

First, principal component analysis effectively discriminated the silenced groups from the control group in both cell lines (online supplemental figure S6A). Online supplemental figure S6B shows cell top differentially expressed peptides after *CNNM4* silencing, with samples primarily organised into groups. The major downregulated pathways predominantly involve metabolic processes, but they also comprise chemotherapeutic processes, inflammatory processes and cancer proliferation and epithelial–mesenchymal transition (EMT) pathways (figure 4A and online supplemental figure S6C). However, the antioxidant system-related pathways were consistently the most affected among the four comparisons, indicating an inhibitory effect of these pathways due to *CNNM4* silencing. All differentially modulated pathways are provided in online supplemental file 3.

NUPR-1, a ferroptosis inhibitor, exhibited the most negative activation z-score as the upstream regulator in *CNNM4*-silenced TFK-1 cells compared with controls (figure 4B). This was confirmed by observing a decrease in NUPR-1 levels and dysregulation of other ferroptosis-associated markers, including GPX-4, ALOX5 and 4-HNE in EGI-1 cells (figure 4C, online supplemental figure S7A,B). Dysregulation of gene expression related to ferroptosis and iron metabolism markers due to *CNNM4* silencing in CCA cells (online supplemental figure S7C) and CCA cell-derived spheroids (online supplemental figure S7D) suggested an enhanced ferroptotic activity, altogether with an increase in iron uptake and storage. No changes in iron metabolism markers in the healthy cholangiocyte H69 cell line after silencing *CNNM4* were observed (online supplemental figure S7E). In contrast, in *CNNM4*-silenced CCA cells, increased intracellular iron levels (figure 4D and online supplemental figure S7F) along with one of the final products of lipid peroxidation, malondialdehyde (MDA) (figure 4E), were detected. Moreover, *CNNM4* silencing in CCA cells resulted in increased mitochondrial ROS (figure 4F and online supplemental figure S7G). Remarkably, patient-derived xenograft models from a cohort of patients with diverse clinical features demonstrated a trend toward a decrease in *CNNM4* positivity in cells harbouring mutated IDH1, known for sensitising cells to ferroptosis (online supplemental figure S7H).²⁶ These findings corroborated the association between reduced *CNNM4* expression and molecular pathways driving ferroptosis.

To understand ferroptosis importance for CCA cells with reduced *CNNM4* expression, cells were exposed to the iron chelator deferiprone. We observed enhanced growth of *CNNM4*-silenced cells (figure 4G), effectively reversing the observed proliferation phenotype. Furthermore, the addition of

zinc protoporphyrin, an inhibitor of heme oxygenase-1 (HO-1), affected the proliferative rate of CCA cells with normal *CNNM4* levels but had no effect on cell growth when *CNNM4* was silenced (figure 4H). Notably, silencing NUPR-1 in CCA cell lines with basal *CNNM4* levels reduced cell proliferation to a similar extent as *CNNM4* silencing and modulated 4-HNE and NUPR-1 protein expression, as well as iron concentration (online supplemental figure S8A–C). In contrast, NUPR-1 overexpression in stable *CNNM4*-silenced CCA cells enhanced cell proliferation and led to a decrease in iron and MDA content (online supplemental figure S8E–H).

In conclusion, ferroptosis is crucial in driving the observed effects in CCA cells when *CNNM4* levels are decreased.

Silencing of *Cnnm4* mitigates tumourigenicity by inducing ferroptosis in a murine model

Based on the obtained data, the AKT/YapS127A sleeping beauty mice model was further employed to shed light on the importance of *CNNM4* for CCA biology (figure 1E).^{19–21} After inducing the tumours, *Cnnm4* was silenced by treatment with *CNNM4*-targeting siRNA conjugated to GalNAc ligand for liver-specific targeting. The AKT/YapS127A sleeping beauty mouse model shows positive immunoreactivity for the asialoglycoprotein receptor 1 (ASGPR1) in both hepatocytes and CCA lesions (online supplemental figure S9A). Additionally, a positive mark was observed by western blot analysis against ASGPR1 in control and CCA mice models (online supplemental figure S9B). In this context, ASGPR1 serves as the receptor for GalNAc-siRNA *CNNM4*. Both CCA-induced groups showed similar echographic manifestations prior to siRNA treatment (online supplemental figure S9C). However, at the time of sacrifice, only the CCA mice treated with siRNA Ctrl demonstrated an increased liver-to-body weight ratio compared with control mice (online supplemental figure S9D).

Based on an independent pathologist's assessment of tumourigenicity, *CNNM4* siRNA-treated mice showed a trend toward a reduction in tumour score. No tumours were detected in other organs of CCA-induced mice. As expected, *CNNM4* immunoreactivity decreased in *CNNM4* siRNA-treated mice (figure 5A), accompanied by reduced transcriptional levels, while other Mg²⁺ transporters' expression remained unchanged (online supplemental figure S9E). Moreover, a decrease in expression of SOX9, GS and epithelial cell adhesion molecule (EpcAM) was observed in tumours excised from *CNNM4* siRNA-treated mice (figure 5A).

In the next step, we aimed to determine the effect of *CNNM4* downregulation on energy metabolism in vivo. Basal glucose levels in control siRNA-treated CCA-induced mice were elevated compared with healthy control and *CNNM4* siRNA-treated CCA-induced mice (figure 5B). Besides, control siRNA treated mice showed increased ECAR in fresh liver tissue (figure 5C) and OCR in freshly isolated mitochondria (figure 5D) in comparison to *CNNM4*-silenced CCA mice.

Concerning ferroptosis, the expression of NUPR-1 and GPX4 was downregulated in *CNNM4*-silenced treated livers (figure 5E and online supplemental figure S9F) with a greater tendency to increased iron and MDA content (figure 5F–H). Finally, immunoreactivity of the key lipid peroxidation by-product 4-HNE was increased in *CNNM4*-silenced livers from animals with CCA, compared with healthy control and control siRNA treated CCA (figure 5I and online supplemental figure S9G).

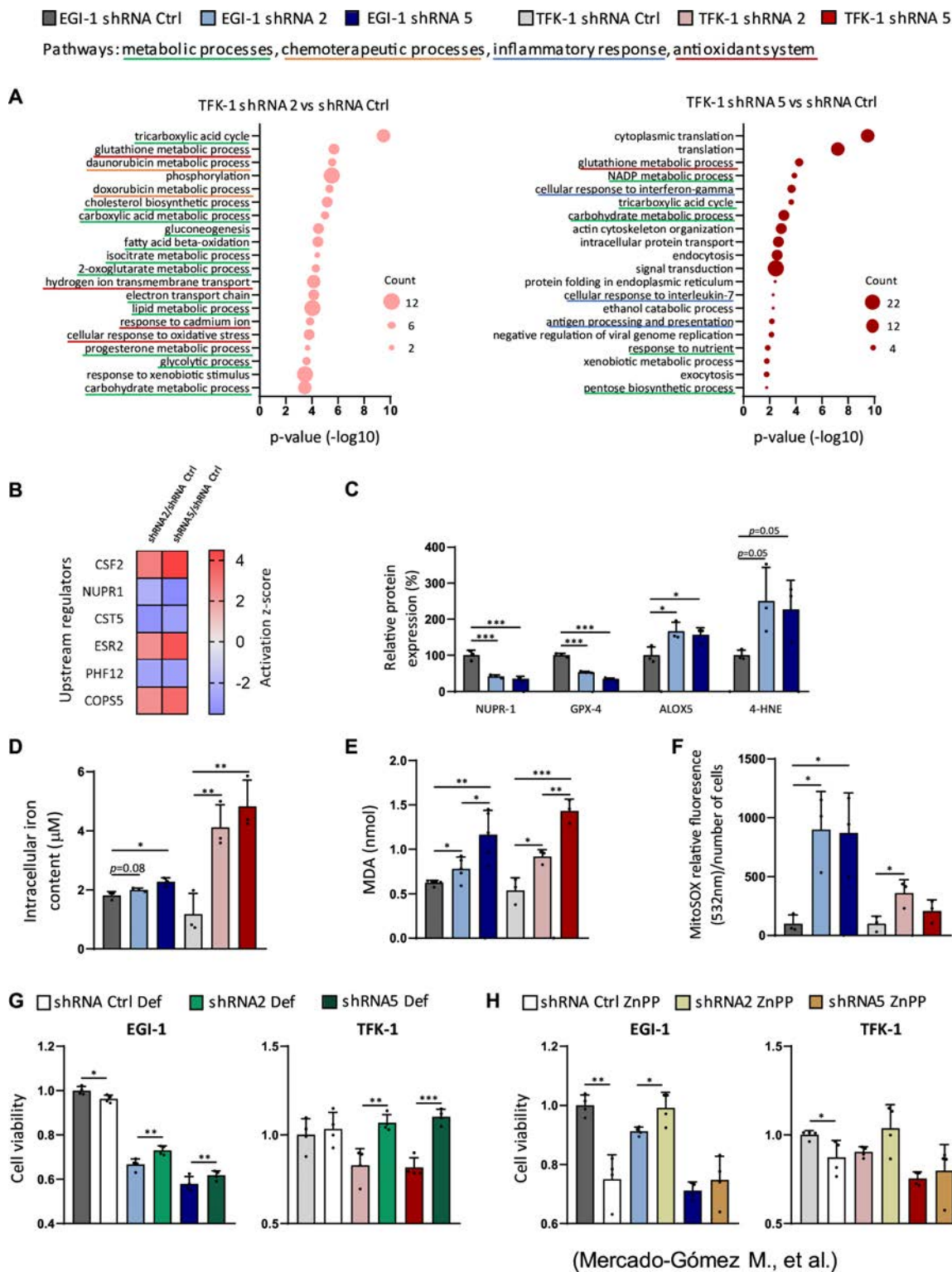
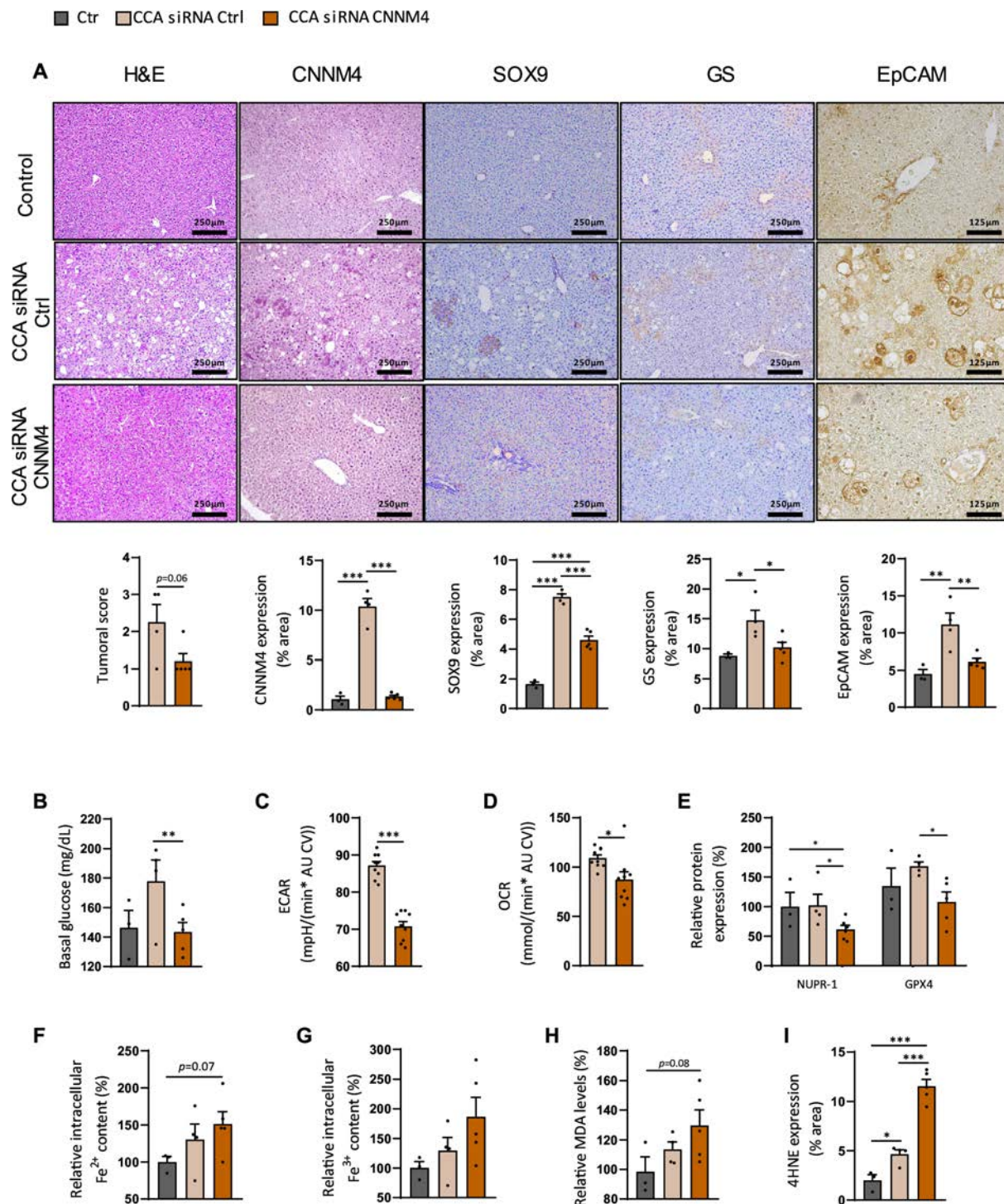


Figure 4 Ferroptosis inhibition in *CNNM4*-silenced CCA cells. (A) Top-20 downregulated gene ontology term-enriched pathways representing the unique differentially expressed peptides in *CNNM4*-silenced TFK-1 compared with control TFK-1 cells ($n=3$). The number of proteins belonging to the identified dysregulated pathways is shown by the diameter measure. (B) Common upstream regulators in TFK-1 cells with *CNNM4* silencing ($n=3$). (C) Protein quantification of NUPR-1, GPX-4, ALOX5 and 4-HNE in stable EGI-1 cells with or without *CNNM4* silencing ($n=3$). (D) Intracellular iron content in CCA cells with *CNNM4* silencing ($n=3$). (E) MDA determination in control and *CNNM4*-silenced CCA cells ($n=5$ in EGI-1 and $n=3$ in TFK-1). (F) Relative MitoSOX fluorescence of the indicated groups ($n=3$). (G) Cell viability after 48 hours treatment with $50\ \mu\text{M}$ deferiprone ($n=4$) in stable EGI-1 cells (*left*) and TFK-1 cells (*right*). (H) Cell viability in stable EGI-1 cells (*left*) and TFK-1 cells (*right*) after 48 hours administration of $25\ \mu\text{M}$ zinc protoporphyrin ($n=4$). Statistical significance was assessed using one-way ANOVA and Student's *t*-test. Error bars represent SD and asterisks indicate *p* values (* <0.05 , ** <0.01 and *** <0.001). ALOX5, arachidonate lipoxygenases 5; ANOVA, analysis of variance; CCA, cholangiocarcinoma; *CNNM4*, cyclin M4; MDA, malondialdehyde; NADP, nicotinamide adenine dinucleotide phosphate; NUPR-1, nuclear protein 1; shRNA, short hairpin RNA; ZnPP, zinc protoporphyrin.



(Mercado-Gómez M., et al.)

Figure 5 Transposon-induced CCA mice model with *CNNM4* silencing showed a less tumorous phenotype. (A) Histological characterisation of *CNNM4*, *SOX9*, *GS* and *EpCAM* in livers from control mice and transposon-induced CCA mice with siRNA control or *CNNM4* treatment and respective quantification. Magnification: 200× and 400×; scale bar: 250µm and 125µm. (B) Glucose levels in serum, (C) ECAR in fresh liver slices and (D) OCR in fresh isolated mitochondria from those mice. (E) *NUPR-1* and *GPX4* protein expression from hepatic homogenates of control mice and untreated and *CNNM4*-silenced CCA-induced mice. Relative determination of ferrous (F), ferric (G) and MDA (H) content in those mice. (I) Immunohistochemical 4-HNE expression in livers from control mice and transposon-induced CCA mice with or without *CNNM4* siRNA treatment. Statistical significance was assessed using one-way ANOVA and Student's t-test. Error bars represent SEM and asterisks indicate p values (* < 0.05, ** < 0.01 and *** < 0.001). ANOVA, analysis of variance; AU CV, arbitrary units from crystal violet quantification; CCA, cholangiocarcinoma; *CNNM4*, cyclin M4; ECAR, extracellular acidification rate; *EpCAM*, epithelial cell adhesion molecule; Fe²⁺, ferrous iron; Fe³⁺, ferric iron; *GPX4*, glutathione peroxidase 4; *GS*, glutamine synthetase; 4-HNE: 4-Hydroxynonenal; MDA, malondialdehyde; *NUPR-1*, nuclear protein 1; OCR, oxygen respiratory rate; siRNA, small interfering RNA.

DISCUSSION

In this study, we have explored the therapeutic potential of targeting CNNM4 as an oncogenic driver in CCA, a malignancy characterised by its aggressive nature and limited treatment options. CNNM4 is consistently upregulated in CCA tumours across both clinical and preclinical samples, distinguishing it as the only transporter from the CNNM family in these contexts.

Mg²⁺ plays a crucial role in cancer physiopathology, contributing to metabolic and physiological functions that can influence carcinogenesis. Epidemiological studies have identified Mg²⁺ deficiency as a risk factor for CCA.¹³ Furthermore, *in vivo* studies demonstrate that animals fed an Mg²⁺-deficient diet developed more lung metastases than controls.²⁷ This could be attributed to the intense inflammatory response triggered by Mg²⁺ deficiency, which may promote cancer progression by fostering the presence of inflammatory cells and mediators in the tumour microenvironment.²⁸ Accordingly, our study reveals that silencing CNNM4 is associated with a decrease in inflammation-related pathways. Moreover, Mg²⁺ is indispensable for activating the nicotinamide adenine dinucleotide phosphate (NADPH) oxidase, a primary source of ROS.²⁹ Conversely, lowering cellular Mg²⁺ has been associated with decreased ROS in a TRPM7 knock-down neuronal model.³⁰ ATP, only active when bound to Mg²⁺, is crucial for iron receptor-mediated endocytosis, as it acidifies the lumen of the endocytic vesicle through the action of H⁺-ATPase, releasing iron from transferrin. Therefore, elevated intracellular Mg²⁺ levels may potentiate iron uptake by the cell, thereby enhancing ROS production via the Fenton reaction.⁷

The effects induced by CNNM4 silencing are interconnected and driven by the increased production of ROS resulting from ferroptosis. Drug resistance has recently been associated with ferroptosis in tumour cells, where iron overload influences the precise ROS homeostasis.³¹ Exposure to drugs like cisplatin triggers ROS production, challenging cell survival. In response, tumour cells activate mechanisms to alter their microenvironment and suppress ROS, leading to drug resistance.³² Ferroptosis plays a crucial role in this process by promoting drug-induced ROS production, thereby increasing the sensitivity of tumour cells to chemotherapeutic treatments.³³ Silencing of CNNM4-induced ferroptosis sensitises CCA cells to commonly used drugs and increases mitochondrial ROS generation, akin to HO-1.³⁴

Chemoresistance is a complex issue in CCA, significantly influenced by CSCs, which have an increased dependence on iron. Iron supplementation promotes CSC-like features in CCA cells, whereas iron chelator treatment impairs spheroid formation.^{33 35} However, maintaining ROS balance is crucial for CSC integrity, since elevated ROS levels damage self-renewal and differentiation and enhance radiotherapy sensitivity.³⁶ Our results demonstrated that baseline CNNM4 levels in CCA cells correlate with enhanced spheroid-forming ability and higher CSC markers, compared with silenced CNNM4 cells. Additionally, in two-dimensional culture, CNNM4-silenced CCA cells exhibit lower CSC marker levels. Consistently, Zhu *et al* demonstrated that FBXO31 promotes cisplatin-induced ferroptosis in CCA and CSC-like cells.³⁷

Regarding CNNM4's role in metastasis, lower CNNM4 levels in CCA cells markedly reduced tissue invasion, vascular migration and lung metastasis in both *ex ovo* and *in ovo* CAM models. Proteomic analysis revealed a downregulation of proliferation, EMT and invasion pathways in CNNM4-silenced CCA cells. Importantly, liver tissue of mice exposed to CNNM4 siRNA exhibited decreased SOX9 and EpCAM immunoreactivity. SOX9 and EpCAM, CSC markers, are associated with cell migration

and invasion through EMT in various cancers.³⁸ Several studies highlighted the vulnerability of cancer cells resistant to conventional treatments or prone to metastasise to ferroptosis.^{39 40} Ferroptosis inversely correlates with metastasis across multiple cancer types, inhibiting cell proliferation, migration and invasion.^{41 42} Similarly, SLC7A11 overexpression is associated with a higher tumour-nodule-metastasis stage and poorer prognosis in human HCC.⁴² Inhibiting the metastasis process may result from ROS-mediated damage, evidenced by 2,2'-dipyridone hydrazone dithiocarbamic acid and HDAC inhibitor.^{43 44}

Finally, silencing of CNNM4 effectively suppressed the Warburg effect in CCA cells, as evidenced by the downregulation of glucose catabolism pathways in TFK-1 cells, possibly influenced by TP53 gene mutations that promote glycolysis in cancer.⁴⁵ EGI-1 cells exhibited decreased oxidative respiration. In our *in vivo* model, mice treated with siRNA for CNNM4 showed reduced serum glucose levels, a known driver of CCA cell proliferation.⁴⁶ Fresh liver and isolated mitochondria from these animals showed less glycolytic and energetic phenotypes, respectively. Recently, CCA has been proposed to depend on mitochondrial oxidative phosphorylation, contributing to the CSC phenotype.⁴⁷ Metabolic reprogramming shares common players with ferroptosis, including glutamate, NADPH, GSH or ROS. Glutaminolysis fuels ferroptosis by converting glutamine to glutamate, essential for the SLC7A11/GSH/GPX4 pathway.⁴⁸ Indeed, GLS2 induces ferroptosis by depleting the available glutamate.⁴⁹ Tricarboxylic acid cycle (TCA) cycle intermediates, including IDH1, linked to ferroptosis, inhibit tumour progression in CCA.⁴ Reduction power is crucial in ferroptosis antioxidant axes and is associated with inhibitors like *de novo* synthesis and fatty acid elongation. Proteomic analysis of CNNM4-silenced cells revealed downregulated NADPH generation involving pentose phosphate pathway and isocitrate conversion to α -KG. Furthermore, during ferroptosis, glycolysis decreases concomitantly with mitochondrial damage caused by oxidative stress, compromising organelle integrity, leading to energy depletion and cell death.⁴³

In brief, cancer cells generate elevated ROS due to their increased metabolic demands. Oxidative stress is a 'double-edged sword' in cancer, as overwhelming levels of ROS make cancer cells more susceptible to death.⁵⁰ Hence, ferroptosis could be a tumour suppressor event in CCA, possibly synergising with other anticancer therapies.⁵¹

Remarkably, in the CCA preclinical mice model, the treatment with GalNAc siRNA CNNM4 significantly reduces the malignancy features in the liver. GalNAc siRNA technology is being successfully evaluated in clinical trials. It offers stability, favourable pharmacokinetics, liver specificity, durable target gene inhibition with infrequent dosing, easy administration and low immunogenicity.⁵² The AKT/YapS127A sleeping beauty mouse model shows positive immunoreactivity for ASGPR1 in both hepatocytes and CCA lesions, indicating that both cell types are potential targets for GalNAc-siRNA CNNM4.

Broadly translated, our findings reveal a novel therapy for CCA: silencing of CNNM4 inhibits progression and growth by reversing key cancer hallmarks. This approach induces ferroptosis-mediated ROS production, enhancing CCA cell sensitivity to chemotherapy, reducing CSC population, halting migration and invasion and preventing metabolic reprogramming alterations. We suggest further investigating GalNAc CNNM4 siRNA as a potent, long-lasting and well-tolerated compound targeting CNNM4 to the liver for treatment of patients with CCA.

Author affiliations

¹Liver Disease Lab, CIC bioGUNE, Basque Research and Technology Alliance (BRTA), Derio, Bizkaia, Spain

²Center for the Study of Liver and Gastrointestinal Diseases (CIBERehd), Carlos III National Institute of Health, Madrid, Spain

³Department of Chemistry and Biochemistry, Mendel University in Brno, Brno, Czech Republic

⁴The Research Institute for Medicines (iMed.Ulisboa), Faculty of Pharmacy, University of Lisbon, Lisbon, Portugal

⁵Proteomics Platform, Bizkaia Science and Technology Park, Derio, Spain

⁶Experimental Hepatology and Drug Targeting (HEVEPHARM), IBSAL, University of Salamanca, Salamanca, Spain

⁷Cancer Cell Signaling and Metabolism Lab, CIC bioGUNE, Basque Research And Technology Alliance (BRTA), Derio, Spain

⁸Ikerbasque Basque Foundation for Science, Bilbao, Spain

⁹Department of Liver and Gastrointestinal Diseases, Biogipuzkoa Health Research Institute, Donostia University Hospital, University of the Basque Country (UPV/EHU), Donostia-San Sebastian, Spain

¹⁰Immunology, Ophthalmology and ENT, Complutense University of Madrid Faculty of Medicine, Madrid, Comunidad de Madrid, Spain

¹¹Hepatology Laboratory Solid Tumors Program CIMA CCUN IdiSNA, Pamplona, Navarra, Spain

¹²Department of Anatomical, Histological, Forensic Medicine and Orthopaedics Sciences, Sapienza University of Rome, Rome, Italy

¹³SilenceTherapeutics GmbH, Berlin, Germany

¹⁴Upper Gastrointestinal and Endocrine Tumor Unit, VHIO, Vall d'Hebron University Hospital, Barcelona, Spain

¹⁵Clinical Research, Vall d'Hebron Institute of Oncology, Barcelona, Spain

¹⁶Department of Biochemistry and Genetics, School of Sciences, University of Navarra, Pamplona, Spain

¹⁷START Madrid-FJD, Hospital Universitario Fundación Jiménez Díaz, Madrid, Spain

¹⁸Medical Oncology, Fundación Jiménez Díaz University Hospital, Madrid, Spain, Madrid, Spain

¹⁹Department of Medicine, David Geffen School of Medicine, Los Angeles, California, USA

²⁰Comprehensive Liver Research Center at University of California, Los Angeles, California, USA

²¹Proteomics Platform, CIC bioGUNE, ProteoRed-ISCIII, Bizkaia Science and Technology Park, Derio, Spain, CIC bioGUNE, Bizkaia, Spain

²²Biochemistry and Molecular Biology, UPV/EHU, Leioa, Spain

²³Department of Chemistry, New York University, New York, New York, USA

²⁴Institute of Pathology, University of Regensburg, Regensburg, Germany

²⁵Medical, Surgical, and Clinical Sciences, University of Sassari, Sassari, Italy

X Isabel Mendizabal @imendizabal1, Maite G Fernandez-Barrena @Maite G Fernandez-Barrena, Rocio I R Macias @rimacias, Victor Moreno @vicmorenogarcia, Angela Lamarca @DrAngelaLamarca, Francisco Javier Cubero @CUBEROLab and Maria Luz Martinez-Chantar @chantar_m

Acknowledgements Plasmids used in animal experiments were kindly supplied by Serge Hardy (McGill University). We are grateful to Jose Juan García Marín's lab (Universidad de Salamanca) and Matías Ávila's lab (CIMA, Pamplona) for providing EGI-1, TFK-1, and H69 cells. We'd also like to thank Arkaitz Carracedo's lab (CICbioGUNE, Bilbao) for supplying HEK293 cells. The GalNaC CNM4 siRNAs molecules were generously provided by ST GmbH. This article is based upon work from the European Network for the Study of Cholangiocarcinoma and the COST Action CA22125 Precision medicine in biliary tract cancer (Precision-BTC-Network) supported by COST (European Cooperation in Science and Technology: www.cost.eu). We also thank MINECO for the Severo Ochoa Excellence Accreditation to CIC bioGUNE (SEV-2016-0644). Special thanks to Arantza Sanz Parra and Begoña Rodríguez Iruretagoyena for the technical support provided.

Contributors MM-G and MLM-C designed the project and wrote the manuscript; MLM-C raised the finding; PO and DB designed experimental protocols; MA and FE performed proteomics analyses; MM-G, NG-U, AEG, MAMR, MBA, LEZ-P, CMR-G, MRR, IM, PMR, IGR, HW, RR-A, MS-M, JAB-B, MGF-B, DO, EG, US, SG-L, MY-B, PP-S, CG-P, AL, HM, ZH, CC, RIRM, TCD, CM, TT, DFC, GC and JJGM contributed to investigations and data analysis; MBA, AC, JB, VM, AL, PS-B, TCD, LAM-C, MAA, RJ, CM, TM, FJC, DFC, GC, JJGM and CMPR contributed to discussions. MLM-C is responsible for the overall content (as guarantor).

Funding This work was supported by grants from Ministerio de Ciencia, Innovación y Universidades MICINN: PID2023- 1469330B-100 funded by MCIU/AEI /10.13039/501100011033/FEDER, UE as part of Plan Estatal de Investigación Científica y Técnica e Innovación (to MLM-C); Grant CEX2021-001136-S funded by MCIU/AEI/10.13039/501100011033 (to MLM-C); Instituto de Salud Carlos III (ISCIII) through the project PMP22/00054 "Exploring the Feasibility of predictive and pharmacodynamics biomarkers of immunotherapy in solid tumors (Immune4ALL)" and co-funded by the European Union; CIBERehd/Project funded by CIBERehd;

La Caixa Banking Foundation under the project code LCF/TR/C123/56000003 (Caixalmpulse) (to MLM-C); Programa Ayudas a proyectos de investigación y desarrollo en salud del Departamento de Salud del Gobierno Vasco (202333041) (to MLM-C); Diputación Foral de Bizkaia dentro del Programa Transferencia Tecnológica 2022 (6/12/TT/2022/00001), co-funded by FEDER (to MLM-C); Proyecto Elkartek, Subvencionado por el Gobierno Vasco (to MLM-C). Ayudas Fundación Científica AECC para proyectos coordinados (IGTP-AECC_2022-042) (for MLM-C); Postdoctoral fellowship JDC2023-052761-I funded by MCIN/AEI (to CMR-G). PhD fellowships from the Scientific Foundation of the Spanish Association Against Cancer PRDV233980ZAPA (to LEZ-P). Ministerio de Ciencia, Innovación y Universidades MICINN: PID2021-126096NB-I005 and RED2018-102379-T and MICINN PID2020-117941RBI00/AEI/10.13039 to FJC); Ministerio de Ciencia e Innovación, Programa Retos-Colaboración RTC2019-007125-1 (for MLM-C); I Ayudas Fundación Científica AECC para proyectos coordinados (IGTP-AECC_2022-042) (for MLM-C); Transferencia tecnológica 2022 (6/12/TT/2022/00001) (for MLM-C); Desarrollo Tecnológico en Salud (DTS20/00138) (for MLM-C); Ayudas a proyectos de investigación y desarrollo en salud (202333041) (for MLM-C); Health Research 2017 (HR17-00601) (for MLM-C) and (LCF/PR/HR21/52410028) (to CMPR); Caixa Impulse Innovation 2023 (CI23-20155) (for MLM-C). OXHEP2-CM (S2022/BMD-7409) and HORIZON-HLTH-2022-STAYHLTH-02 under agreement No 101095679 (for FJC). EG, DO and GC were supported by PNRR M4C2- Investimento 1.4- CN00000041" Funded by the European Union – NextGenerationEU, Project PNC 0000001 D3 4 Health, - CUP B53C22006120001, The National Plan for Complementary Investments to the NRRP, Funded by the European Union – NextGenerationEU, and PRIN 2022 (20222J7W2K). DB acknowledges support of National Cancer Institute of the National Institutes of Health under award number R01CA127817. Spanish Ministry of Science and Innovation (Proyectos de Generación de Conocimiento 2022: PID2022-1402100B-I00) (for M.R.R.); Fondo de Investigaciones Sanitarias, Instituto de Salud Carlos III, Spain, co-funded by the European Regional Development Fund/European Social Fund, "Investing in your future" (PI22/00526 for JJGM, and PI23/00681 for RIRM); "Junta de Castilla y León" (SA113P23) (for JJGM); AECC Scientific Foundation (2023/2027) (for JJGM). JMB received funds from Spanish Carlos III Health Institute (ISCIII) [(FIS PI21/00922, PI18/01075 and Miguel Servet CPII19/00008)] cofunded by the European Union. Diputación Foral Gipuzkoa" (2020-CIEN-000067-01, 2021-CIEN000029-04-01 and 2023-CIEN-000008-01 to PMR). Department of Health of the Basque Country (2022111070 to P.M.R.). Fundação para a Ciência e a Tecnologia, Portugal (PTDC/MEDFAR/3492/2021) (to CMPR). Personal fellowships: MM-G (FPI, PRE2018-084840); LEZ-P (AECC, PRDV233980ZAPA); PP-S (FPI, PRE2021-097073); M-G-F-G (Ramon y Cajal Program contract, RYC2018-024475-1); PMR (FIS PI23/01850, Sara Borrell CD19/00254 and Miguel Servet CP22/00073).

Competing interests None declared.

Patient and public involvement Patients and/or the public were not involved in the design, or conduct, or reporting, or dissemination plans of this research.

Patient consent for publication Consent obtained directly from patient(s).

Ethics approval Immunohistochemistry analyses performed in ENS-CCA cohort was approved by Ethic Committee of Euskadi, Spain (Code: PI2016137). Immunohistochemistry analyses performed in Regensburg cohort was approved by Ethical Committee of the University Medicine of Greifswald. Participants gave informed consent to participate in the study before taking part.

Provenance and peer review Not commissioned; externally peer reviewed.

Data availability statement All data relevant to the study are included in the article or uploaded as supplementary information.

Supplemental material This content has been supplied by the author(s). It has not been vetted by BMJ Publishing Group Limited (BMJ) and may not have been peer-reviewed. Any opinions or recommendations discussed are solely those of the author(s) and are not endorsed by BMJ. BMJ disclaims all liability and responsibility arising from any reliance placed on the content. Where the content includes any translated material, BMJ does not warrant the accuracy and reliability of the translations (including but not limited to local regulations, clinical guidelines, terminology, drug names and drug dosages), and is not responsible for any error and/or omissions arising from translation and adaptation or otherwise.

Open access This is an open access article distributed in accordance with the Creative Commons Attribution Non Commercial (CC BY-NC 4.0) license, which permits others to distribute, remix, adapt, build upon this work non-commercially, and license their derivative works on different terms, provided the original work is properly cited, appropriate credit is given, any changes made indicated, and the use is non-commercial. See: <http://creativecommons.org/licenses/by-nc/4.0/>.

ORCID iDs

Maria Mercado-Gómez <http://orcid.org/0000-0003-2765-6432>

Maite G Fernandez-Barrena <http://orcid.org/0000-0003-0375-6236>

Diletta Overi <http://orcid.org/0000-0003-3561-8903>

Saioa Garcia-Longarte <http://orcid.org/0000-0001-5412-4234>
 Rocio I R Macias <http://orcid.org/0000-0002-4748-0326>
 Victor Moreno <http://orcid.org/0000-0001-6099-4236>
 Matias A Avila <http://orcid.org/0000-0001-6570-3557>
 Tian V. Tian <http://orcid.org/0000-0002-9906-0980>
 Francisco Javier Cubero <http://orcid.org/0000-0003-1499-650X>
 Guido Carpino <http://orcid.org/0000-0001-8570-2519>
 Jose J G Marin <http://orcid.org/0000-0003-1186-6849>
 Maria Luz Martinez-Chantar <http://orcid.org/0000-0002-6446-9911>

REFERENCES

- Ali H, Tedder B, Waqar SH, et al. Changing incidence and survival of intrahepatic cholangiocarcinoma based on Surveillance, Epidemiology, and End Results Database (2000–2017). *Ann Hepatobiliary Pancreat Surg* 2022;26:235–43.
- Elgenidy A, Afifi AM, Jalal PK. Survival and Causes of Death among Patients with Intrahepatic Cholangiocarcinoma in the United States from 2000 to 2018. *Cancer Epidemiol Biomarkers Prev* 2022;31:2169–76.
- El-Diwanly R, Pawlik TM, Ejaz A. Intrahepatic Cholangiocarcinoma. *Surg Oncol Clin N Am* 2019;28:587–99.
- Su L, Huang Y, Zheng L, et al. Isocitrate dehydrogenase 1 mutation in cholangiocarcinoma impairs tumor progression by sensitizing cells to ferroptosis. *Open Med* 2022;17:863–70.
- Stockwell BR. Ferroptosis turns 10: Emerging mechanisms, physiological functions, and therapeutic applications. *Cell* 2022;185:2401–21.
- Yan H, Zou T, Tuo Q, et al. Ferroptosis: mechanisms and links with diseases. *Sig Transduct Target Ther* 2021;6:1–16.
- Liu J, Song X, Kuang F, et al. NUPR1 is a critical repressor of ferroptosis. *Nat Commun* 2021;12.
- Huang C, Santofimia-Castaño P, Iovanna J. NUPR1: A Critical Regulator of the Antioxidant System. *Cancers (Basel)* 2021;13:3670.
- Sui M, Jiang X, Chen J, et al. Magnesium isoglycyrrhizinate ameliorates liver fibrosis and hepatic stellate cell activation by regulating ferroptosis signaling pathway. *Biomed Pharmacother* 2018;106:125–33.
- Jahnen-Dechent W, Ketteler M. Magnesium basics. *Clin Kidney J* 2012;5:i3–14.
- Shah SC, Zhu X, Dai Q, et al. Magnesium intake is associated with a reduced risk of incident liver cancer, based on an analysis of the NIH-American Association of Retired Persons (NIH-AARP) Diet and Health Study prospective cohort. *Am J Clin Nutr* 2021;113:630–8.
- Liu M, Yang H, Mao Y. Magnesium and liver disease. *Ann Transl Med* 2019;7:578.
- Zhong G-C, Peng Y, Wang K, et al. Magnesium intake and primary liver cancer incidence and mortality in the Prostate, Lung, Colorectal and Ovarian Cancer Screening Trial. *Int J Cancer* 2020;147:1577–86.
- Ko HJ, Youn CH, Kim HM, et al. Dietary Magnesium Intake and Risk of Cancer: A Meta-Analysis of Epidemiologic Studies. *Nutr Cancer* 2014;66:915–23.
- Hardy S, Uetani N, Wong N, et al. The protein tyrosine phosphatase PRL-2 interacts with the magnesium transporter CNNM3 to promote oncogenesis. *Oncogene* 2015;34:986–95.
- Kostantin E, Hardy S, Valinsky WC, et al. Inhibition of PRL-2-CNNM3 Protein Complex Formation Decreases Breast Cancer Proliferation and Tumor Growth. *J Biol Chem* 2016;291:10716–25.
- González-Recio I, Simón J, Goikoetxea-Usandizaga N, et al. Restoring cellular magnesium balance through Cyclin M4 protects against acetaminophen-induced liver damage. *Nat Commun* 2022;13:6816.
- Simón J, Goikoetxea-Usandizaga N, Serrano-Maciá M, et al. Magnesium accumulation upon cyclin M4 silencing activates microsomal triglyceride transfer protein improving NASH. *J Hepatol* 2021;75:34–45.
- Fan B, Malato Y, Calvisi DF, et al. Cholangiocarcinomas can originate from hepatocytes in mice. *J Clin Invest* 2012;122:2911–5.
- Wang J, Wang H, Peters M, et al. Loss of Fbxw7 synergizes with activated Akt signaling to promote c-Myc dependent cholangiocarcinogenesis. *J Hepatol* 2019;71:742–52.
- Zhang S, Song X, Cao D, et al. Pan-mTOR inhibitor MLN0128 is effective against intrahepatic cholangiocarcinoma in mice. *J Hepatol* 2017;67:1194–203.
- Afzal MS, Pitteloud JP, Buccella D. Enhanced ratiometric fluorescent indicators for magnesium based on azoles of the heavier chalcogens. *Chem Commun (Camb)* 2014;50:11358–61.
- Qin H, Zheng G, Li Q, et al. Metabolic reprogramming induced by DCA enhances cisplatin sensitivity through increasing mitochondrial oxidative stress in cholangiocarcinoma. *Front Pharmacol* 2023;14:1128312.
- Raggi C, Taddei ML, Rae C, et al. Metabolic reprogramming in cholangiocarcinoma. *J Hepatol* 2022;77:849–64.
- Izquierdo-Sanchez L, Lamarca A, La Casta A, et al. Cholangiocarcinoma landscape in Europe: Diagnostic, prognostic and therapeutic insights from the ENSCCA Registry. *J Hepatol* 2022;76:1109–21.
- Serra-Camprubi Q, Verdaguer H, Oliveros W, et al. Human Metastatic Cholangiocarcinoma Patient-Derived Xenografts and Tumoroids for Preclinical Drug Evaluation. *Clin Cancer Res* 2023;29:432–45.
- Nasulewicz A, Wietrzyk J, Wolf FI, et al. Magnesium deficiency inhibits primary tumor growth but favors metastasis in mice. *Biochimica et Biophysica Acta* 2004;1739:26–32.
- Mazur A, Maier JAM, Rock E, et al. Magnesium and the inflammatory response: potential physiopathological implications. *Arch Biochem Biophys* 2007;458:48–56.
- Aoyagi K, Takeshige K, Sumimoto H, et al. Role of Mg²⁺ in activation of NADPH oxidase of human neutrophils: evidence that Mg²⁺ acts through G-protein. *Biochem Biophys Res Commun* 1992;186:391–7.
- Chen H-C, Su L-T, González-Pagán O, et al. A key role for Mg(2+) in TRPM7's control of ROS levels during cell stress. *Biochem J* 2012;445:441–8.
- Zhang C, Liu X, Jin S, et al. Ferroptosis in cancer therapy: a novel approach to reversing drug resistance. *Mol Cancer* 2022;21:47.
- Okon IS, Zou M-H. Mitochondrial ROS and cancer drug resistance: Implications for therapy. *Pharmacol Res* 2015;100:170–4.
- Nie Z, Chen M, Gao Y, et al. Ferroptosis and Tumor Drug Resistance: Current Status and Major Challenges. *Front Pharmacol* 2022;13:879317.
- Kongpetch S, Kukongviriyapan V, Prawan A, et al. Crucial role of heme oxygenase-1 on the sensitivity of cholangiocarcinoma cells to chemotherapeutic agents. *PLoS ONE* 2012;7:e34994.
- Recalcati S, Gammella E, Cairo G. Dysregulation of iron metabolism in cancer stem cells. *Free Radic Biol Med* 2019;133:216–20.
- Cosialls E, El Hage R, Dos Santos L, et al. Ferroptosis: Cancer Stem Cells Rely on Iron until "to Die for" It. *Cells* 2021;10:2981.
- Zhu Z, Zheng Y, He H, et al. FBXO31 sensitizes cancer stem cells-like cells to cisplatin by promoting ferroptosis and facilitating proteasomal degradation of GPX4 in cholangiocarcinoma. *Liver Int* 2022;42:2871–88.
- Yuan X, Li J, Coulouarn C, et al. SOX9 expression decreases survival of patients with intrahepatic cholangiocarcinoma by conferring chemoresistance. *Br J Cancer* 2018;119:1358–66.
- Tsoi J, Robert L, Paraiso K, et al. Multi-stage Differentiation Defines Melanoma Subtypes with Differential Vulnerability to Drug-Induced Iron-Dependent Oxidative Stress. *Cancer Cell* 2018;33:890–904.
- Hangauer MJ, Viswanathan VS, Ryan MJ, et al. Drug-tolerant persister cancer cells are vulnerable to GPX4 inhibition. *Nature New Biol* 2017;551:247–50.
- Nagpal A, Redvers RP, Ling X, et al. Neoadjuvant neratinib promotes ferroptosis and inhibits brain metastasis in a novel syngeneic model of spontaneous HER2⁺ breast cancer metastasis. *Breast Cancer Res* 2019;21:94.
- He Q, Liu M, Huang W, et al. IL-1 β -Induced Elevation of Solute Carrier Family 7 Member 11 Promotes Hepatocellular Carcinoma Metastasis Through Up-regulating Programmed Death Ligand 1 and Colony-Stimulating Factor 1. *Hepatology* 2021;74:3174–93.
- Guan D, Li C, Li Y, et al. The DpdtbA induced EMT inhibition in gastric cancer cell lines was through ferritinophagy-mediated activation of p53 and PHD2/hif-1 α pathway. *J Inorg Biochem* 2021;218:111413.
- Oliveira T, Hermann E, Lin D, et al. HDAC inhibition induces EMT and alterations in cellular iron homeostasis to augment ferroptosis sensitivity in SW13 cells. *Redox Biol* 2021;47:102149.
- Zhang C, Liu J, Liang Y, et al. Tumour-associated mutant p53 drives the Warburg effect. *Nat Commun* 2013;4:2935.
- Saengboonmee C, Seubwai W, Pairojkul C, et al. High glucose enhances progression of cholangiocarcinoma cells via STAT3 activation. *Sci Rep* 2015;6:18995.
- Raggi C, Taddei ML, Sacco E, et al. Mitochondrial oxidative metabolism contributes to a cancer stem cell phenotype in cholangiocarcinoma. *J Hepatol* 2021;74:1373–85.
- Liu Y, Lu S, Wu L, et al. The diversified role of mitochondria in ferroptosis in cancer. *Cell Death Dis* 2023;14:519.
- Suzuki S, Venkatesh D, Kanda H, et al. GLS2 Is a Tumor Suppressor and a Regulator of Ferroptosis in Hepatocellular Carcinoma. *Cancer Res* 2022;82:3209–22.
- Perillo B, Di Donato M, Pezone A, et al. ROS in cancer therapy: the bright side of the moon. *Exp Mol Med* 2020;52:192–203.
- Yang M, Li M, Lyu Z, et al. Implication of Ferroptosis in Cholangiocarcinoma: A Potential Future Target? *Cancer Manag Res* 2023;15:335–42.
- Springer AD, Dowdy SF. GalNAC-siRNA Conjugates: Leading the Way for Delivery of RNAi Therapeutics. *Nucleic Acid Ther* 2018;28:109–18.